A First Principles Exploration of a Variety of Active Surfaces and Catalytic Sites in Ziegler−Natta Heterogeneous Catalysis

Mauro Boero,*,‡,|| Michele Parrinello,† Horst Weiss,§ and Stephan Hüffer§

Max-Planck-Institut für Festkörperforschung, Heisenbergstrasse 1, D-70569 Stuttgart, Germany, Joint Research Center for Atom Technology (JRCAT), Angstrom Technology Partnership (ATP), 1-1-4 Higashi, Tsukuba, Ibaraki 305-0046, Japan, and Polymer Research Division, BASF Aktiengesellschaft, D-67056 Ludwigshafen, Germany

Received: February 28, 2001

We present a Car−Parrinello investigation of various active surfaces and catalytic sites in a realistic Ziegler−Natta heterogeneous system. We examine the (100), (110), and (104) surfaces of the $MgCl_2$ support and the related binding of the possible mononuclear and dinuclear catalyst configurations. Relaxation and/or reconstruction processes affect these surfaces in varying degrees, according to the different Miller indexes. We find that $TiCl_4$ and Ti_2Cl_6 species can bind as stable adducts, depending on the morphology of the surface considered. However, the activation and polymerization phases show that destabilization phenomena can affect the dinuclear species during the catalysis reaction. This provides a new insight into the ability of the different centers to give rise to the real polymerization process. Finally, we present a first attempt to address the role of a typical donor phthalate at a fully first principles level.

1. Introduction

The problem of the polymerization process in heterogeneous catalysis is a question arising directly from industry, aiming to address improvements and rational developments in polyolefin production.

It is well-known that Ziegler−Natta (ZN) catalysis[1,2] is one of the most important industrial processes in the mass production of polyolefins with a high degree of stereoselectivity. In particular, heterogeneous catalysis mantains a leading role in industry because of its economical advantages. So far, unfortunately, very little is known experimentally about the nature of the active centers, their local geometry, and the related electronic structure. Experimental probes suffer severe limitations, since only a relatively low percentage of the catalytic sites are active, and, as a consequence, their local structure and electronic properties are not known with any great certainty. Modeling the catalytic ability of different centers at the best level allowed by the present state-of-the-art of quantum simulations, may thus be the only systematic way of obtaining the needed insight.

As far as heterogeneous catalysis is concerned, these theoretical investigations are only now becoming possible. This is mainly due to the complexity of such a system, which prevented realistic calculations in past years. Development of new computational techniques as well as remarkable progress in computer facilities have now made it possible to study large realistic systems in great detail.

In a standard preparation of a magnesium chloride/titanium chloride catalytic system, the milling process of $MgCl_2$ can produce different active surfaces on which the Ti can coordinate in several ways.[3−7] Since these Ti configurations can strongly differ in their stereoselective properties, the control of these surfaces is a crucial issue in tuning the polymer stereochemistry. Experimental investigations generally focus on the analysis of the polymer produced and correlations with the catalyst preparation are done at a second stage in order to recover a microscopic picture with the aid of model structures.[8−10]

On the theoretical front, some of these catalyst configurations have been extensively investigated by Corradini and co-workers,[8,9] using assumed geometries of both the substrate and the catalytic center. However, due to the size of the system needed to reproduce a realistic environment, ab initio calculations have so far been prohibitively expensive. For this reason simplified approaches have been adopted. Paired interacting orbital (PIO) calculations[12] on a number of violet $TiCl_3$ configurations have been reported by Shiga et al.;[13] of course they do not deal with the $MgCl_2$ substrate problem and do not account for relaxation problems. Semiempirical approaches of the extended Hückel type have been reported[14] on crystalline $TiCl_3$ clusters, but the need for more sophisticated theoretical methods is acknowledged by the authors themselves. Various support surfaces have been studied by Colbourn et al.[15] using molecular modeling methods combined with density functional (DFT) calculations. However, their DFT studies were limited to inclusion of surface fragments treated at a first principles level into structures computed classically using two-body model potentials. First principles calculations limited to static relaxation of Ti adducts and all-electron calculations on smaller cluster models have recently been reported by Gale and co-workers;[16] however, their outcome is limited since a realistic model is not used for the polymerization process, temperature and dynamical effects are not accounted for, binding energies are unrealistically low (some of them are indeed at the limits of the accuracy allowed by first principles calculations), and all the Ti catalyst models reported in the very rich literature have been neglected.

In our previous works[17,18] we have already investigated the basic aspects of the polymerization of both ethylene and

† Max-Planck-Institut für Festkörperforschung.
‡ JRCAT−ATP.
§ BASF Aktiengesellschaft.
|| Work done at MPI−FKF, Stuttgart (Germany).

10.1021/jp010780d CCC: $20.00
Published on Web 05/04/2001

propylene in a realistic ZN system. In this paper we extend our study to the most representative support surfaces, i.e., (100), (110), and (104) whose active Mg sites include a great variety of possible undercoordinated Mg configurations. We analyze the various Ti geometries, starting from the most accredited models proposed by Corradini and co-workers[8] to the 5-fold site reported in ref 17. Here we find that also a dinuclear form of this same center can exist as a stable configuration prior to the activation.

We study then, for the first time in a realistic system, the effects of the activation and the polymerization reaction on these catalyst configurations, in the attempt to elucidate the problem of their relative stability and their contribution to the polymerization process. Our results show that the ability of a center to carry out its catalytic role without being destabilized, depends to a large extent on the nature of the center and its geometrical environment.

Furthermore, we discuss the problem of the regioselectivity of the proposed 5-fold site, an issue that was left open in our previous work,[18] and present a first attempt to address the role of a donor phthalate in the ZN system.

2. Computational Method

We adopted a DFT[19] approach with gradient corrections on exchange and correlation after Becke−Lee−Yang−Parr (BLYP)[20] and performed Car−Parrinello[21] simulations[22] using supercells containing: 30 formula units in an orthorombic supercell of 17.673 × 14.560 × 28.000 Å^3 in the case of (100) surface, 32 formula units in a monoclinic supercell of 19.095 × 12.522 × 28.000 Å^3 ($\widehat{ab}$ = 70.2°) in the case of (110) surface, and 48 formula units in an orthorombic supercell of 14.560 × 21.711 × 28.000 Å^{3}in the case of (104) surface.[23]

These choices ensure a thickness sufficient to simulate the bulk, a surface realistically large and enough empty space above the surface to avoid interactions with periodic images. Catalyst centers are separated by at least 14.560 Å from their replicas in the (*x*,*y*) directions in the case of the smaller cell; the separation along *z* is of course the third dimension of the supercells. The atoms are fixed to the bulk crystallographic positions on one side of the slab, while the catalytic centers are placed on the opposite (relaxed) side. Troullier−Martins[24] norm-conserving pseudopotentials including nonlinear core corrections[25] for Mg and Ti accounted for the valence−core interactions. A plane wave expansion with an energy cutoff of 70 Ry (= 952.41 eV = 35.0 au) was adopted unless otherwise specified in the text.[26] This higher cutoff was needed to describe the oxygen properties. Pseudopotential convergence tests concerning the choice of the cutoff have been reported elsewhere.[17] In the case of the open-shell calculations, local spin density approximation (LSDA) on exchange and correlation within the same BLYP functional was adopted. The choice of a BLYP functional approach is clearly driven by the fact that at the simple LDA level binding energies turn out to be overestimated and the insertion barrier largely underestimated or completely missed.[17] Of course, the choice of the functional is not unique and the general agreement, especially of energetics, is expected to depend strongly on the level at which exchange and correlation are treated. We used a BLYP version according to our experience with several systems, ranging from hydrogen-bond systems to organometallics[27] and to the extensive comparative tests reported in the literature[28] where it is shown that the performances of BLYP are comparable to (or sometimes slightly better than) the Perdew correlation functional family more popular in the homogeneous catalysis simulation field.

As in our previous works,[17,18] for the olefin insertion reactions, we performed constrained molecular dynamics within the Blue Moon ensemble theory,[29,30] assuming as the reaction coordinate the distance between the incoming olefin and the α-carbon of the growing polymer chain. Equilibration times of ∼2.0 ps ensured sufficiently meaningful statistics. Free energies are affected by an average error bar of about 2.0 kcal/mol within our choice of the exchange and correlation functional.

3. Active Surfaces

The $MgCl_2$ crystal has already been described elsewhere.[17] Here we recall only the main points needed to support the following discussion. Solid $MgCl_2$ has an ionic layered structure which belongs to the $R\bar{3}m$ space group. We took the experimental geometry[31] and optimized the lattice parameter *a* consistently with our DFT approach. The *c* lattice constant was fixed to the experimental value since along this direction van der Waals forces, not well described by any class of density functionals, play the major role. Our optimized *a* bulk value was 3.651 Å, which differs from the experiment (3.640 Å) by about 0.3%. The Mg−Cl bond length of the relaxed structure is 2.520 Å, in good agreement with the experimental value of 2.530 Å[32]. Starting from this optimized structure, we cleaved the different surfaces as described in the following paragraphs.

Even if the (001) surface is supposed to be prevalent in a standard substrate preparation, this surface is not interesting from a practical point of view, since it is the basal plane of the crystal. For this reason it is easy to cleave $MgCl_2$ along this plane, where only relatively weak van der Waals forces hold the structure together, but surfaces obtained in this way are completely saturated by Cl and not catalytically active. They can be activated by removing Cl atoms by, for example, electron irradiation.[33] These experiments are rather clever and allow fine control of both the surface and the active sites. However, this aspect of the problem is beyond the scope of the present work and this is not the technique generally adopted in industry.[34]

3.1. (100) Surface. We started our analysis by considering the (100) surface, quoted in the literature[8,35] as a good active surface for coordinating epitactically the chiral dinuclear Ti_2Cl_6 species.

When the (100) surface is cleaved from the α-$MgCl_2$ bulk crystal, the structure of the three exposed layers of the elementary cell is such that one of them (left layer of Figure 1a) presents all 6-fold Mg atoms, i.e., the layer is Cl terminated, the neighboring layer (central layer of Figure 1a) exposes 3-fold Mg atoms, and the third layer (right layer in Figure 1a) shows 5-fold Mg sites. The fact that one of the layers of the exposed surface is highly undercoordinated (3-fold) makes this initial configuration very unstable. In fact, due to the large charge imbalance, Coulomb forces acting between two adjacent layers induce remarkable reconstruction processes. Both simple structure relaxation and free molecular dynamics have shown that the chlorine atoms of the 6-fold Mg layer jump toward the neighboring layer in the attempt to balance the surface net charges. Eventually, a further displacement of these Cl along this same layer leads to the formation of new Mg−Cl bonds, resulting in a structure where all the layers expose a 5-fold coordinated Mg (Figure 1b). The total energy gain of this reconstruction process is 12.7 kcal/mol Mg.[36]

It is interesting to observe that if β-$MgCl_2$ is used instead of α-$MgCl_2$, the (100) surface is much closer to the reconstructed one described above, thus a less dramatic relaxation process occurs.

3.2. (110) Surface. A description of the relaxation of this surface has already been given in a previous work,[17] where a

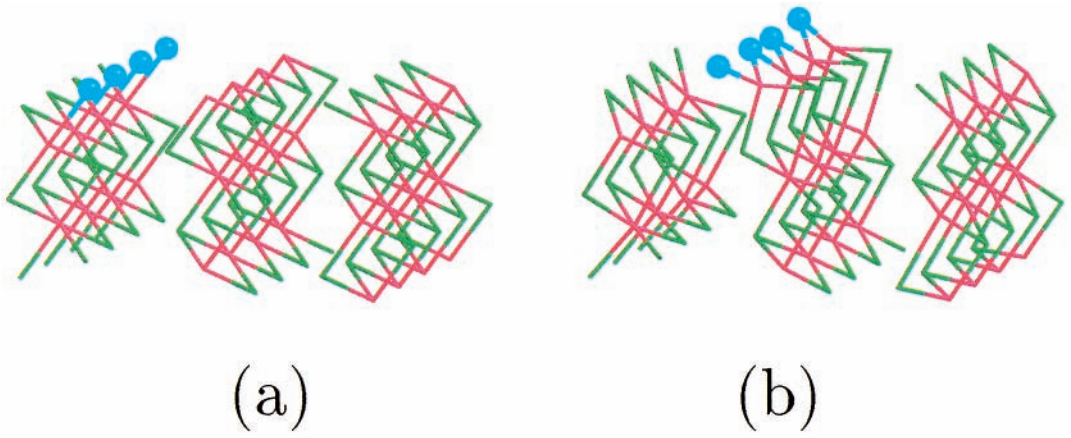

Figure 1. (100) surface of $MgCl_2$. The initial surface (a) as cleaved from the bulk reconstructs as in (b) in less than 0.4 ps during a constant energy molecular dynamics. Mg atoms are represented by the cross points of the pink stick segments while the green parts refer to the Cl atoms. For the sake of clarity, the Cl atoms jumping from the left 6-fold layer to the next one are shown as light blue balls. Here and in the following figures only the portion of the system close to the surface is shown, the real dimensions being those reported in the computational details section.

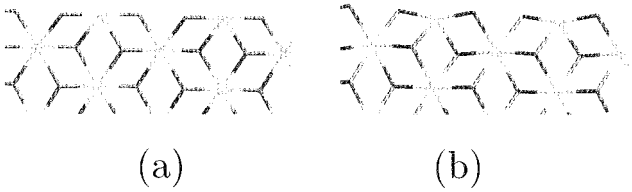

Figure 2. Details of the (110) surface (a) prior to and (b) after the relaxation process leading to the puckering of the exposed Mg atoms toward the bulk. The structure is represented by sticks only where the Mg atoms are located at the cross points of the light gray stick segments. Cl atoms are the darker segments.

slightly smaller cell was adopted. In the present calculation, the supercell has been enlarged as explained in the computational details section. This, however, does not affect the relaxation process, so we limit our analysis to a brief summary of the main points. A (110) surface cleaved from the bulk shows layers which are all terminated by 4-fold Mg sites (Figure 2a). In this case the relaxation does not give rise to any reconstruction, but only to a puckering of the Mg atoms on the surface toward the bulk (Figure 2b). The 180° typical bulk angle of Cl−Mg−Cl reduces to 154° on the surface while the Mg−Cl bond lengths shorten to 2.403 and 2.322 Å. The energy gain of the process for the simulated system amounts to 3.4 kcal/mol Mg.

3.3. (104) Surface. This surface, as cleaved from the bulk, presents only 5-fold Mg active sites and is very *flat* compared to the previous ones. The active surface is very similar, from the coordination point of view, to the reconstructed (100). The relaxation affects the structure only a little and the global effect is a small puckering of the exposed Mg atoms toward the bulk without any change in coordination. The flat Cl−Mg−Cl bulk angle reduces to 162.1° and the Mg−Cl bonds at the surface stretch to to 2.421 and 2.597 Å from the bulk values reported above. The effects of the relaxation are shown in Figure 3a (unrelaxed) and Figure 3b (relaxed). The total energy gain in this case was 2.4 kcal/mol Mg.

The general picture that emerges from these calculations is that the active surfaces of $MgCl_2$ are such that only two coordinations are allowed for Mg: either 5-fold or 4-fold. Lower coordination numbers would result in much less stable lateral cuts. This provides a justification for the assumptions given in the literature[8] where only (100) and (110) are considered by speculating on similarities with the violet $TiCl_3$. In what follows we shall focus on the binding of different catalyst configurations onto (100) and (110) surfaces, not because these are the only possible exposed surfaces, but because they are representative of all the stable Mg configurations and correspond to the lowest possible Miller indices, i.e., to the energetically less expensive lateral cuts. Of course, since in real experiments the milling

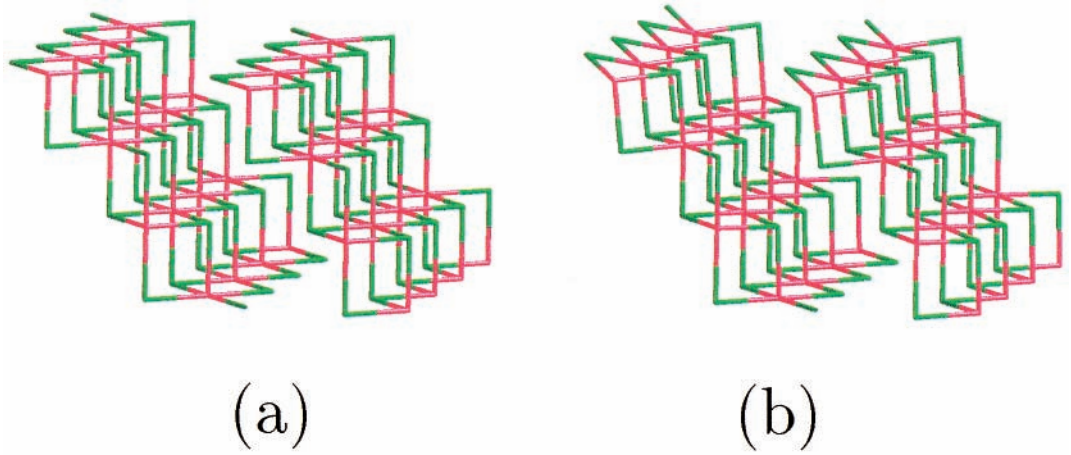

Figure 3. Details of the relaxation of the (104) surface. Being an extremely flat cut, the cleaved structure (a) reverts to (b) showing only a slight modification with respect to the unrelaxed one. The color code of the segments is the same as in Figure 1, i.e., Mg are in pink and Cl in green.

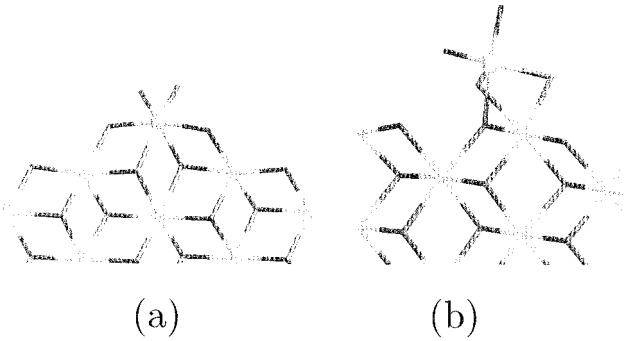

Figure 4. Corradini's mononuclear Ti adduct (a) and 5-fold Ti configuration (b) on the (110) surface. Both structures are fully relaxed. No stable mononuclear species could be located on other surfaces. The $MgCl_2$ substrate is indicated by sticks as in Figure 2. The Ti atom is shown as a ball on top of the surfaces.

procedure can expose different $MgCl_2$ cuts, in view of these results it is irrelevant to specify the actual surface of the support.

4. Binding of Ti Catalyst on the Active Surfaces

4.1. $TiCl_4$. Purely mononuclear species on surfaces such as (100) or (104), where only 5-fold Mg are present, have been supposed to form as a consequence of the dissociation of dinuclear Ti adducts.[8] However, in our calculations, mononuclear catalytic sites on these surfaces were never found stable at any stage, i.e., neither prior to nor after the activation. In all our simulations, attempts to stick a $TiCl_4$ molecule on the relaxed (100) surface failed. A simple static relaxation of the system gave a very weak binding of about 2.0 kcal/mol—indeed at the cutting edge of first principles accuracy—but as soon as dynamics was allowed, the Ti adduct was rapidly destabilized and the $TiCl_4$ flew away as a free molecule.

We found that stable $TiCl_4$ geometries are allowed only on the (110) surface, where the lower Mg coordination number favors their binding. We have already discussed the possible $TiCl_4$ configurations on this surface.[17] Here we limit our analysis to a brief summary of these geometries and their relevant binding energies. The most popular model is the Corradini configuration reported in Figure 4a. The binding energy of this Ti 6-fold is 40.3 kcal/mol. An alternative possibility is a 5-fold site like the one shown in Figure 4b, whose binding energy is lower (29.4 kcal/mol) due to the fact that the Ti coordinates to the substrate with one bond less than the Corradini center. Both species become active ZN sites, the 5-fold one being characterized by a higher reactivity.

The energetics for the propelne insertion at the 5-fold site has been discussed in a previous paper[18]. For the sake of completeness, we will briefly recall the main features here. The site was proved to be stable under polymerization conditions and the formation of a π-complex occurred in a barrierless way with a complexation energy of 3.6 kcal/mol. The computed activation barrier of 10.8 kcal/mol was in agreement with experimental activation energies relevant to the regular 1,2 insertion. A figure of merit was the natural—i.e., without stereomodifiers—stereoselectivity of this site.

For the Corradini-center (see Figure 4a), we assumed a Ti(III) active species in which one of the two dangling Cl atoms is removed while the other one is replaced by a methyl group. This is the simplest model for the active center carrying the growing polymer chain. The π-complexation again is exothermic, the activation barrier is higher by about 7.1 kcal/mol with respect to the 5-fold species. A detailed discussion on this site and the fact that it is not stereoselective in the absence of extra-ligands in the vicinity was already given by Busico and coworkers in ref 9. For this reason, we did not perform further calculations on it.

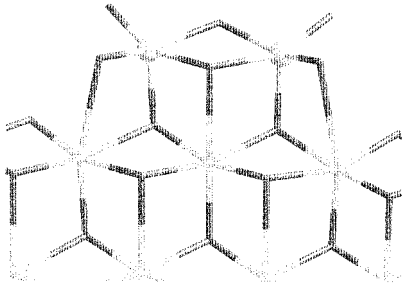

Figure 5. Fully relaxed Corradini's dinuclear Ti adduct on the (100) surface. Energetics and geometrical details are given in the text. The Ti atoms are indicated as balls.

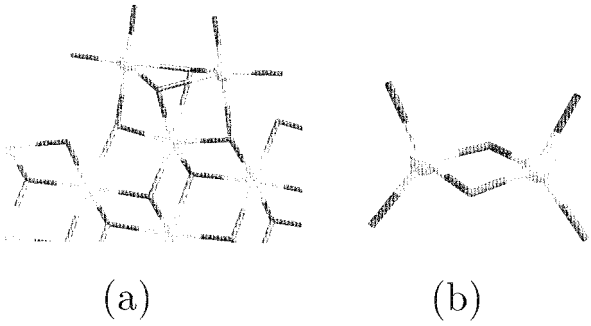

Figure 6. Dinuclear Ti center on the (110) surface (a) obtained via unconstrained constant energy molecular dynamics by simulating the deposition of a Ti_2Cl_4 molecule (b) on the relaxed surface of Figure 2b.

4.2. Ti_2Cl_6. Dinuclear species models have been proposed by the group of Corradini[8] In their original formulation, these centers are suitably bound to surfaces on which the Mg is 5-fold coordinated, as in the case of (100) and (104) cuts. In our calculations we focused on the (100) only, since it is representative of each 5-fold terminated surface. Indeed, we found that a dinuclear structure binds to the substrate with 5 bonds and is characterized by a binding energy of 55.6 kcal/mol. The relaxed Ti_2Cl_6 configuration is shown in Figure 5. The Ti_2Cl_6 adduct forms 5 bonds with the substrate, whose equilibrium distances are Ti−Cl = 2.375 Å, Cl−Mg = 2.673 Å (central bond of the Ti dinuclear species in Figure 5), and Cl−Mg = 3.065 Å (the two lateral bonds in Figure 5); the large distance of the lateral bonds is already symptomatic of a weak binding of the dinuclear adduct which will have important consequences on the stability of the site in the polymerization process, as will be discussed in the following paragraphs. The bond stress affecting the dinuclear Ti species can be ascribed to the mismatch between the Mg−Mg distance (3.674 Å) on the (100) cut of the support and the Ti−Ti distance of Ti_2Cl_6. In fact, the geometry of the gas-phase molecule (Figure 6b) is such that the Ti−Ti distance is 2.870 Å, thus significantly shorter than the Mg−Mg separation, while the molecular Ti−Cl bond are 2.384 Å and 2.233 Å for the Cl bridging the two Ti and the dangling Cl, respectively. Hence, large deformations and bond elongations are required for a Ti dinuclear adduct to stick on the (100) surface.

As suggested by M. Terano,[37] one may speculate that a more efficient binding on (100) can be achieved by *islands* of Ti, like, e.g., Ti atoms trapped below the Ti dinuclear adduct and substituting part of the Mg of the substrate. This could have the advantage of gradually smoothing out the lattice mismatch from the bulk to the surface, allowing for a more stable dinuclear

Ti center. However, this goes far beyond the scope of the simulations presented here.

On the other hand, the possibility of a Ti_2Cl_6 adduct on the (110) surface has to the best of our knowledge never been considered before. Following the unbiased approach that allowed us to identify the 5-fold site, i.e., deposition of a molecule from the gas phase onto the support, we found that a dinuclear species can stick on this surface in the stable configuration shown in Figure 6a, the geometry of which is simply a distortion of the molecular structure of the Ti_2Cl_6 molecule (Figure 6b). The Ti_2Cl_6 molecule sticks on the surface forming 4 bonds and is characterized by a geometry very similar to the afore-described 5-fold center. The two Ti−Cl distances to the support are 2.469 Å, while the two Cl atoms bridging the two Ti form very weak bonds (2.995 Å) with the exposed Mg of the surface. In this case the binding energy is 33.6 kcal/mol, much lower than the dinuclear adduct on (100).

5. Complexation and Polymerization Reaction

5.1. Mononuclear Ti Species (2,1 insertion). The reactivities and relevant stabilities of the mononuclear configurations have already been reported elsewhere.[17] Here we address the question of the regioselectivity by investigating the 2,1 insertion in the alkylated 5-fold center, an issue that was left open in a previous work.[18]

In this sole case, we use an energy cutoff of 40 Ry (= 544.23 eV = 20.0 au). Since these calculations do not involve oxygen, the lower cutoff is sufficient to ensure a good convergence and allows for direct comparison with the calculations of ref 18. We recall that for this site, the stereoregular 1,2 insertion occurs with a barrierless complexation and that from the π-complex to the transition state leading to the isotactic insertion, a barrier of 10.8 kcal/mol has to be overcome, in agreement with experimental findings.[40,41] The total energy gain, from the complex to the product, turned out to be 16.7 kcal/mol and the role of the substrate was similar to that of the bulky ligands in metallocene catalysis.[42]

If a 2,1 insertion is attempted on this same site, a stable π-complex cannot be located by simple geometry optimization or free dynamics. In fact, the reversed position of the large CH_3 group gives rise to strong steric interactions with the Cl atoms around the Ti center (see Figure 7a). The complex was obtained only by a constrained dynamics approach, where the distance $\xi = |\mathbf{R}(C_1) - \mathbf{R}(Ti)|$ between the Ti and the C_1 atom of the carbon double bond of the incoming propene was gradually reduced. The complexation barriers were found to be $\Delta E = 6.7$ kcal/mol and $\Delta F = 5.6$ kcal/mol for the total and free energy, respectively. For a complexation process, this is a rather large barrier and it is due to the partial destabilization of the Ti center. In fact, the Ti adduct loses a bond with the substrate and weakens its binding to the support (see Figure 7b,c). Once the complex is formed and the constraint ξ released, the structure remains stable without reverting to the original configuration.

From this complex, assumed as a reference level, we located, via constrained molecular dynamics, a transition state reported in Figure 7d and energetically located at $\Delta E = 27.7$ kcal/mol and $\Delta F = 16.2$ kcal/mol, much higher than the insertion barrier for the isotactic channel. In this case, the reaction coordinate ξ was chosen to be the distance between the C_2 atom of the propene and the C_α of the growing polymer chain, $\xi = |\mathbf{R}(C_2) - \mathbf{R}(C_\alpha)|$, using the labeling of Figure 7c. The large total energy value is not entirely due to the entropic contribution but also to the weakening of the bonds between the catalyst and the support. The entropic contribution is, however, very large because of the great flexibility of the Ti-polymer chain-monomer group which is only weakly bound to the support and thus can oscillate quite freely and reorient itself. The two dangling chlorines bound only to Ti and visible in Figure 7c are also characterized by very large oscillations. Of course, this very floppy structure is far from being a stable catalytic center. We located this transition state as usual in the framework of the Blue Moon theory, by looking for the zero of the constraint force[30] along the selected reaction path. We further checked this point by performing a vibrational analysis, within the harmonic approximation, on the average configuration as obtained from the trajectory, finding one imaginary mode $\omega = i137$ cm^{-1}.

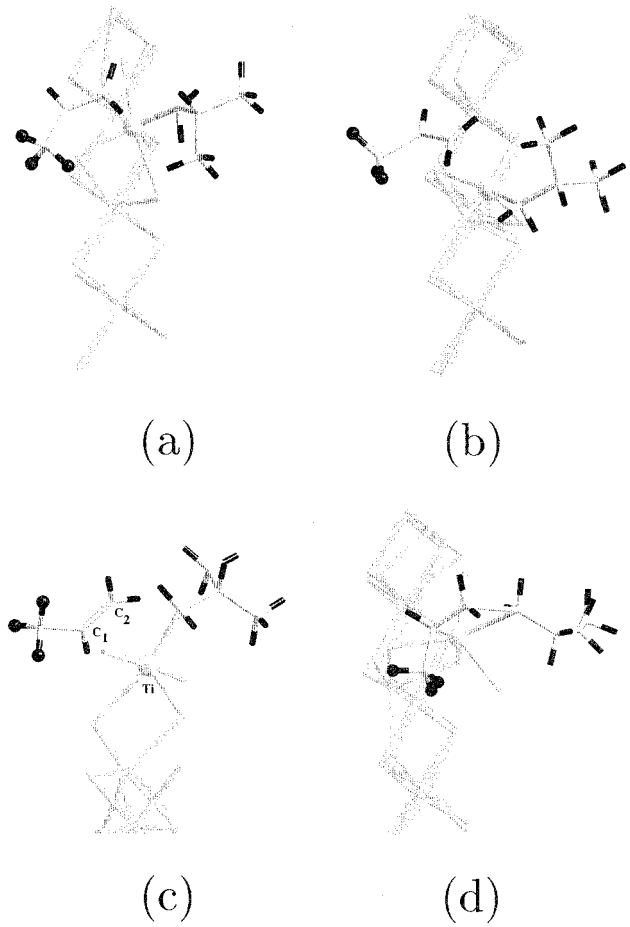

Figure 7. The various phases of the 2,1-insertion. Without loss of generality, the propene is *si*-coordinated throughout all calculations. The approaching of a propene to the 5-fold Ti active center on (110) surface from a top view (a), the π-complex formed after overcoming an activation barrier as reported in the text (top view (b) and side view (c)) and the transition state (d). The olefin−catalyst equilibrium distances for the complex are Ti−C_1 = 3.101 Å and Ti−C_1 = 2.939 Å. (c) the transition state (top view). The equilibrium geometry of this four-membered ring transition structure, averaged from the dynamical run, is: $C_1-C_2 = 1.471$ Å, $C_2-C_\alpha = 2.301$ Å, Ti−C_1 = 2.295 Å, and Ti−C_α = 2.598 Å. The Ti is the gray ball at the center of each panel, while C_α is the C of the polymer chain directly bound to Ti. For the sake of clarity, atomic labels are indicated only in (c).

This result is in line with the conclusions drawn in ref 18 and indicates that the stereoselective channel is favored also in comparison with the 2,1 insertion. Thus, as found in experiments, regioerrors are characterized by a very low probability for this site, whose symmetry is C_1.[9]

5.2. Dinuclear Ti Species. As far as dinuclear Ti configurations are concerned, to the best of our knowledge, no first principles calculations have ever been attempted previously. To

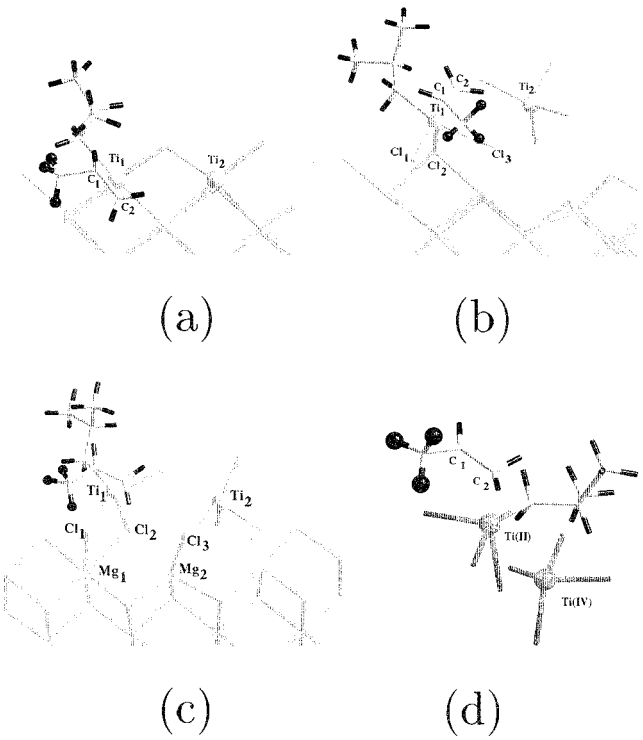

Figure 8. Approach of a propene (top view) to the activated dinuclear Ti center on (100) surface (a) and stable π-complex formed in a barrierless way (b). (c) shows the complexation of a propene on the same dinuclear center in a triplet spin state and (d) the cluster model used to analyze the triplet instability in terms of orbital Hessian (see text for details).

study the ability of the dinuclear species to carry out the polymerization, we simulated the alkylated center by substituting one of the dangling Cl atoms with an isobutyl group and by simulating the complexation of a propene on the active site. For the (100) surface, this is shown in Figure 8a. The complexation proceeds in a barrierless way. However, after performing an unconstrained dynamics, we observed a spontaneous disruption of the dinuclear species with one $TiCl_4$ being expelled as in Figure 8b, and the formation of a stable π-complex on Ti_1. Note that in Figure 8b Ti species revert to a 4-fold coordination, in line with our findings that it is not possible to have a stable mononuclear species on the (100) surface.

The actual Ti oxidation state resulting after this destabilization deserves some comment. The expelled molecule is of course Ti(IV). On the Ti_1 atom, on the other hand, the propene unit forms a stable complex with equilibrium distances $Ti_1-C_1 = 3.104$ Å and $Ti_1-C_2 = 2.372$ Å. But it loses almost all its bonds with the substrate and survives as a Ti(II) species. As a matter of fact, the equilibrium bond distances of Ti_1 turn out to be $Ti_1-Cl_1 = 2.291$ Å, $Ti_1-Cl_2 = 2.498$ Å, $Ti_1-Cl_3 = 2.530$ Å, and $Ti_1-C_\alpha = 2.273$ Å where the labeling is reported in Figure 8c. As can be inferred from these bond lengths, only Cl_1 and C_α atoms can be regarded as chemically bound to Ti_1, the former being mostly ionic and the latter mostly covalent, thus accounting for its formal oxidation state.

We inspected the electronic structure of the Ti(II) species in order to figure out if a Ti-olefin π^* back-donation process occurs. The ELF (electron localization function)[43] shown as a density map in Figure 9a seems to point to a rather different electron distribution, with a strong σ-like component in the π-complex pointing toward the Ti(II) site. This picture is confirmed also by the analysis of the Kohn−Sham orbitals (see Figure 9b). In a full Dewar−Chatt−Duncanson process, the carbon double bond of the olefin is generally aligned to the Ti(II) in such a way that the two carbon atoms labeled as C_1 and C_2 in Figure 8b are symmetrically located and their relative distances from the catalyst are roughly the same. In this case, on the contrary, we find the two distances strongly inequivalent, being $Ti(II)-C_1 = 3.104$ Å and $Ti(II)-C_2 = 2.372$ Å. From the electronic point of view, in the case of a back-donation a Ti-olefin $\pi-\pi^*$ interaction should be observed. Here, however, this is not the case, since the Cl atoms around the catalyst, namely Cl_1 and Cl_3 in Figure 8b give rise to a strong steric repulsion with the methyl group of the propene. Hence, only C_2 can approach Ti(II) in an efficient way, thus forming the σ-like bond visible in Figure 9. Hence, a back-donation process

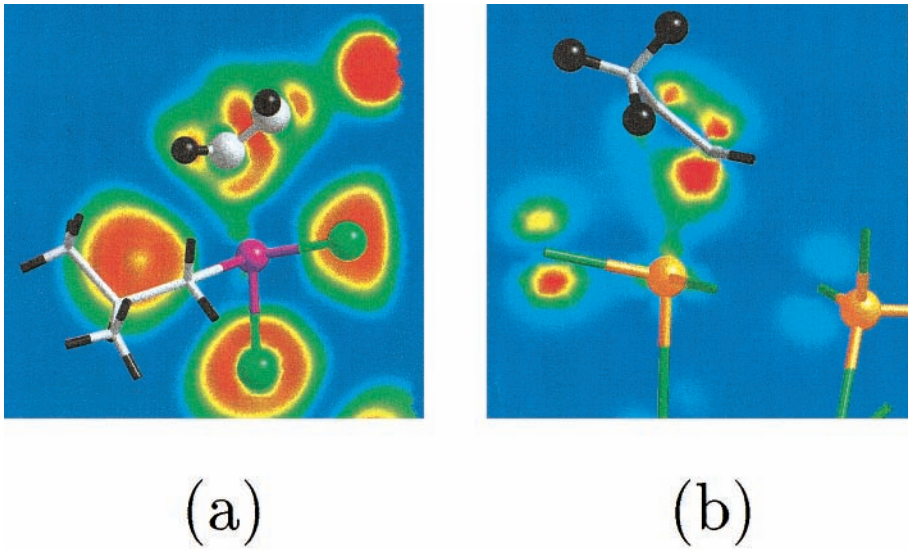

Figure 9. (a) Detail of the electron localization function (ELF) relevant to the complex Ti(II)−propene. The ELF is projected onto the plane defined by the two atoms of the carbon double bond (gray balls) and the Ti(II) (here represented as a purple ball). Red spots are the region of maximum localization (ELF = 1), blue regions refer to the absence of electronic charge (ELF = 0). The green balls are Cl atoms and the polymer chain is represented by sticks only (H in black). Mg atoms are not visible. (b) Kohn−Sham orbital relevant to the propene−Ti(II) σ-like bond. The Ti atoms are here shown as a yellow sphere, while the other colors are the same as in (a). Ti(II) is the one on the left carrying the propene complex. The orientation is reversed with respect to (a) for clarity of presentation.

with a propene, whose steric encumbrance is larger than ethylene, seems to be hindered in a heterogeneous system.

The whole destabilization process is energetically downhill and leads to a total energy gain of 55.8 kcal/mol. The observed disproportionation $2Ti(III) \rightarrow Ti(IV) + Ti(II)$ could be also a consequence of the closed shell ansatz, which is justified, since the singlet is lower in energy than the triplet.

We performed analogous calculations on an open shell triplet state of this same Ti dinuclear configuration in order to check whether the spin state of the system can affect the stability of this species. Also in this case, however, the final structure exhibits a large destabilization with the dinuclear adduct broken into two fragments, a Ti(III) carrying the complex and a Ti(III) weakly bound to the substrate, as shown in Figure 8c. The Cl_1 and Cl_2 atoms bridging the Ti_1 and the substrate are still bound to Mg_1 with bond lengths $Cl_1-Mg_1 = 2.664$ Å, $Cl_1-Ti_1 = 2.374$ Å, $Cl_2-Mg_1 = 2.683$ Å, and $Cl_2-Ti_1 = 2.465$ Å. The only Cl atom connecting Ti_2 to the substrate (Cl_3) has equilibrium distances $Cl_3-Mg_2 = 2.555$ Å and $Cl_3-Ti_2 = 2.430$ Å. The complex itself is still stable as the two propene−catalyst distances are $Ti_1-C_1 = 3.033$ Å and $Ti_1-C_2 = 2.595$ Å.

The final (destabilized) states of this complex have shown a singlet−triplet splitting of 19.5 kcal/mol, the triplet being the energetically higher state.

To further verify the above conclusions, we checked the stability of the structure by computing the orbital Hessian of both the singlet (broken symmetry solutions) and the triplet (lower lying unrestricted solutions). Since this is a feature generally not available in any plane wave code, we extracted from the average configuration of the system undergoing the dynamics the smaller model sketched in Figure 8d. This model includes only the chemically relevant part of the system. A single point DFT calculation within the same BLYP approach used in all present simulations was performed with the DSCF program of the package TURBOMOLE[44], followed by a stability check calculation with the ESCF program of this same package. No negative eigenvalues were found. This clearly confirms that the solutions obtained for the larger periodic system is stable and that the disproportionation is not an artifact of the assumed ansatz.

On these grounds, we can argue that the destabilization of dinuclear species is symptomatic of all those surfaces, like the reconstructed (100) or the (104), on which the exposed Mg is 5-fold.

We checked in an analogous way the stability of the dinuclear adduct on the (110) surface. The alkylation was achieved by substituting a dangling Cl atom of one of the two Ti atoms with an isobutyl group in a way similar to the dinuclear Ti on (100). Also in this case the formation of a stable π-complex (equilibrium distances: $Ti_1-C_1 = 2.185$ Å, $Ti_1-C_2 = 2.162$ Å) as a response to an incoming propene occurs with a destabilization of the dinuclear species. In fact, the Ti carrying the complex (Ti_1) loses all the bonds with the neighbor Ti_2 and keeps only the Cl_1 atom as a binding to the substrate. The equilibrium bond lengths of this bridging Cl are $Ti_1-Cl_1 = 2.521$ Å and $Mg_1-Cl_1 = 2.413$ Å (see Figure 10). This bridging Cl, originally belonging to the substrate, loses one of its bonds (Mg_2-Cl_1), so that the complex survives as a Ti(II) fragment weakly attached to the support. It is interesting to observe that Ti_2does not leave the surface as in the (100) case, but remains bound to the support in a Ti(IV) 5-fold configuration identical to the mononuclear 5-fold center. It is worth speculating that the Ti_2Cl_6 species might act on the (110) surface as a precursor of the mononuclear 5-fold site. The whole process is characterized by an energy gain of 69.2 kcal/mol, roughly of the same order as the value found for the (100) surface. Even in this case, for the actual polymerization process dinuclear centers seem unable to carry out the reaction without destabilizing.

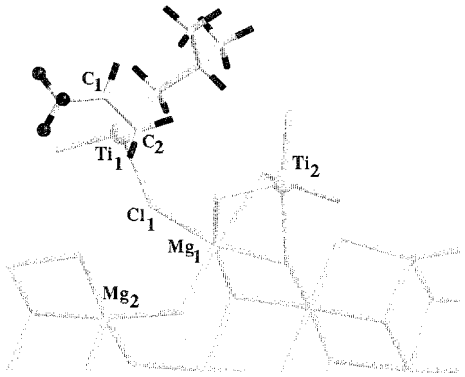

Figure 10. Stable π-complex on the active dinuclear Ti center on the (110) surface. See text for details.

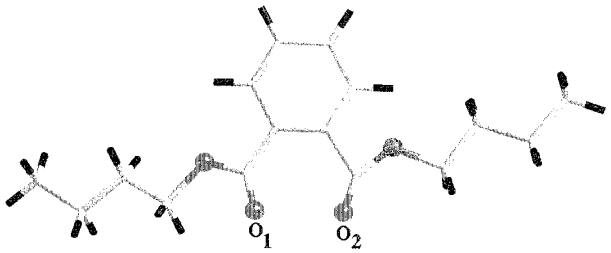

Figure 11. The donor di-*n*-butyl phthalate used in our calculation. The oxygen atoms are shown as balls, C atoms are the light gray sticks and H atoms the black sticks. O_1 and O_2 are the oxygen atoms that interact with the active surfaces.

On these grounds, we can conclude that dinuclear centers, at least in these catalyst configurations, although stable prior to the activation, do not remain stable when the polymerization occurs, contrary to the mononuclear Ti configurations, which, to this extent, can be identified as a real active catalyst.

6. The Donor Di-*n*-butyl Phthalate

As a first attempt to address the role of an internal donor in a $MgCl_2/TiCl_4$ catalytic system (i.e., a donor added during the preparation of the catalyst), we considered the prototype molecule reported in Figure 11, which is representative of a whole family of internal donors. The results presented here can then be regarded as rather general. These kinds of phthalates, of which the di-*n*-butyl phthalate is a quite common species, are known to improve the degree of stereoselectivity[35] and are generally designed in order to fulfill the following requisites: (i) ability to coordinate on the $MgCl_2$ support also in the presence of Ti adducts, (ii) absence of secondary reactions with Ti during the catalyst preparation, (iii) absence of secondary reactions with both the metal−carbon bond and the growing polymer chain during the polymerization process. Requisite (i) is generally achieved by tuning the O_1-O_2 distance of the molecule in the range 2.7−3.8 Å while the other two aspects depend on the particular molecular structure, as well as the influence of external donors added during the polymerization process and are the object of intensive research in the molecular design domain.[35] In this respect, this part of our work was done in the same spirit as ref 35(e) where diethers are considered and attempts are made to correlate the binding of the donors

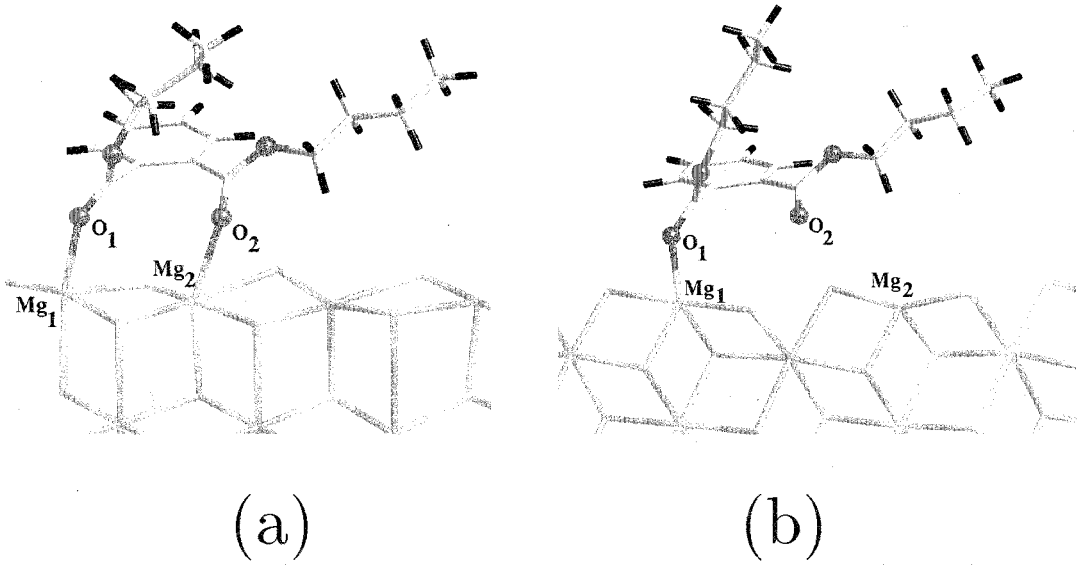

Figure 12. (a) Equilibrium configuration of the donor phthalate bound to the (100) surface. (b) Binding of the donor phthalate on the (110) surface. Due to the surface geometry, only one bond can be formed in this case. Binding energies and equilibrium bond distances are reported in the text.

on the various surfaces to the isospecificity of the produced polymer. Both phthalates and diethers are used at the stage of catalyst preparation and are supposed to behave in a similar way. Unfortunately, despite intensive investigation, their role is still unclear.

The di-*n*-butyl phthalate is a rather floppy molecule and, due to the flexibility of the hydrocarbon chains, the O_1-O_2 distance can vary very easily in the range 3.370−3.761 Å, because the two hydrocarbon branches carrying the O atoms can reorient freely upon dynamics. The Mg−Mg distance of the exposed Mg on the relaxed active surface is equal to 3.674 Å and 6.360 Å for the (100) and (110) cuts, respectively. It is then clear that such a donor can bind very efficiently on (100), while a less strong binding can be expected on (110). In fact, calculations for the (100) surface gave a binding energy of 21.9 kcal/mol with bond distances $O_1-Mg_1 = 2.150$ Å and $O_2-Mg_2 = 2.246$ Å for the relaxed structure reported in Figure 12a.

On (110) surface, we performed two simulations. In the first one the donor phthalate was allowed to move freely on the surface searching for stable coordinations. In the second one we started with a relaxed bidentate configuration, according to the models proposed in the literature.[35] In both cases the stable configuration was found to be a singly bonded structure, like the one reported in Figure 11b. In fact, when dynamics is allowed and temperature effects enter the game, a bidentate donor coordination spontaneously loses a bond with the surface and reverts to a single-bond coordination. The bonds of a bidentate configuration, at least for this donor phthalate, are indeed rather stretched, thus this finding is not so surprising. Due to the larger Mg−Mg distance on (110) with respect to (100), the donor can form easily only one bond with the surface, as shown in Figure 12b. The binding energy is 8.5 kcal/mol and the bond length $O_1-Mg_1 = 2.085$ Å. This bond almost restores the local geometry of Mg_1 to the bulk values, the Mg_1-Cl surface distances being now equal to 2.456 Å and the angle $Cl\widehat{Mg}Cl = 177.0°$ very close to the 180° value typical of the bulk crystal.

It might be speculated that the role of such a donor is that of a tuning agent able to control the surface morphology, in the sense that its strong binding on (100)—or, more generally, on surfaces exposing 5-fold Mg—prevents crystal growths exposing these surfaces and enhances or at least does not appreciably affect the (110) cuts. The lower binding of this molecule to (110), also in comparison with the binding energies of Ti adducts, in fact makes it easy to displace this donor and replace it with Ti active centers.

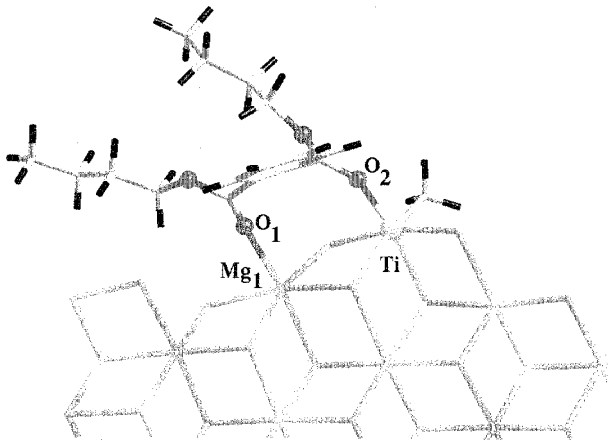

Figure 13. Poisoning of the active Corradini mononuclear center on the (110) surface by the donor phthalate. Details are given in the text.

On the other hand, we found that this same donor phthalate can bind to the activated mononuclear Corradini center with a binding energy of 20.1 kcal/mol, very similar to the binding of the same phthalate on the (100) bare surface. This is not surprising, since, in this case, the distance $Ti-Mg_1$where the donor binds (see Figure 13) is 3.781 Å, very close to the Mg−Mg distance of a typical (100) surface. The equilibrated phthalate−catalytic center bond distances are $O_1-Mg_1 = 2.203$ Å and $Ti-O_2 = 1.942$ Å. This strong binding indicates that mononuclear Corradini centers not carrying the side ligands described in ref 9 are easily poisoned by these donors and in their presence they cannot carry out the polymerization process.

In the case of the 5-fold centers on this same surface, the distance between the Ti and the nearest undercoordinated Mg is much larger than the possible O_1-O_2 distances and a binding of the phthalate is not possible. As a consequence, 5-fold sites are not affected by its presence and can polymerize without being deactivated.

7. Conclusions

We presented an extensive investigation of a realistic Ziegler−Natta heterogeneous system at the cutting edge of present day first principles methodology. We provided well assessed grounds to support the widely made assumption that (100) and (110) are the relevant active surfaces of the $MgCl_2$ support. Indeed, these represent the most stable undercoordinations of the exposed Mg.

The results of the calculations on the catalyst configurations clearly indicate that the proposed active centers on surfaces such as (100) or (104), where the Mg is 5-fold coordinated, are not able to carry out the polymerization process efficiently. On these surfaces, Ti adducts can bind only in a dinuclear configuration, but the catalyst is destabilized during the reaction.

An alternative dinuclear configuration as a possible active site could be located on (110) surface, but it turns out to destabilize as well during the polymerization phase. However, on (110) cuts the mononuclear species act as stable active sites.

It is worthy of note that the destabilization of the dinuclear adduct on this surface leaves the system with a stable 5-fold mononuclear configuration, i.e., contrary to the other cases, here the nonactivated part of the adduct does not fly away as a free $TiCl_4$ molecule, but remains bound to the surface, strengthening the importance of the role of the 5-fold site.

These results are novel and indicate that the simple models and more approximate treatments reported in the literature are insufficient to take into account all the complexity of a ZN heterogeneous catalyst and need to be critically reexamined. In particular, the privileged role that the (100) cut was previously assumed to have, also in comparison with the (110) cut seems to be unfounded. On the basis of our calculations, it can be concluded that the Ti in mononuclear form should be the dominant species in the real catalysis process for simple adducts, unless more complicated structures, which cannot a priori be excluded, are considered.

Our study also presents a first attempt to clarify the role of a typical donor phthalate at a fully first principles level. This is a dual role; on one hand it controls the surface morphology by blocking the growth of those cuts, like (100) and (104), where the 5-fold Mg does not bind Ti efficiently and favoring the (110). On the other hand, it poisons centers such as the Corradini one which, due to the C_2 symmetry, does not have the right stereoselective properties. Also this is new and could not be found via more simplified approaches.

We believe that this work provides new insight for a rational improvement of the heterogeneous catalytic process.

Acknowledgment. We are grateful to Kiyoyuki Terakura, Pier Luigi Silvestrelli, Yoshitada Morikawa, and John Lynch for fruitful discussions and precious suggestions as well as BASF Aktiengesellschaft and TARGOR for financial support.

References and Notes

(1) Ziegler, K.; Holzkamp, E.; Breil, H.; Martin, H. *Angew. Chem.* **1954**, *67*, 541.

(2) Natta, G. *Macromol. Chem.* **1955**, *16*, 213.

(3) See, e.g., (a) *Ziegler Catalysts*; Fink, G., Mülhaupt, R., Brintziger, H. H., Eds.; Springer-Verlag: Heidelberg, 1994. (b) *Progress and Development of Catalytic Olefin Polymerization*; Sano, T., Uozumi, T., Nakatani, H., Terano, M., Eds.; Technology and Education Pubs.: Tokyo, 2000.

(4) Soga, K.; Shiono, T.; Doi, Y. *Makromol. Chem.* **1988**, *189*, 1531.

(5) Terano, M.; Kataoka, T.; Keii, T. *J. Polym. Sci. A* **1990**, *28*, 2035.

(6) (a) Keii, T.; Suzuki, E.; Tamura, M.; Murata, M.; Doi, Y. *Makromol. Chem.* **1982**, *183*, 2285. (b) Keii, T.; Terano, M.; Kimura, K.; Ishii, K. In *Transition Metals and Organometallics as Catalysts for Olefin Polymerization*; Kaminsky, W., Sinn, H., Eds.; Springer-Verlag: Berlin, 1988; p 3.

(7) Pino, P.; Mülhaupt, R. *Angew. Chem.* **1980**, *92*, 869, and references therein.

(8) (a) Corradini, P.; Busico, V.; Guerra, G. *Monoalkene Polymerization: Stereospecificity* in *Comprehensive Polymer Science* **1988**, *4*, 29−50. (b) Busico, V.; Corradini, P.; De Martino, L.; Proto, A.; Savino, V. *Makromol. Chem.* **1985**, *186*, 1279. (c) Busico, V.; Cipullo, R.; Corradini, P.; De Biasio R. *Macromol. Chem. Phys.* **1995**, *196*, 491. (d) Cavallo, L.; Guerra, G.; Corradini, P. *J. Am. Chem. Soc.* **1998**, *120*, 2428.

(9) (a) Busico, V.; Corradini, P.; De Martino, L.; Proto, A.; Albizzati, E. *Makromol. Chem.* **1986**, *187*, 1115. (b) Busico, V.; Cipullo, R.; Monaco, G.; Talarico, G.; Vacatello, M.; Chadwick, J. C.; Segre, A. L.; Sudmeijer, O. *Macromol.* **1999**, *32*, 4173.

(10) (a) Han-Adebekun, G. C.; Ray, W. H. *J. Appl. Polym. Sci.* **1997**, *65*, 1037. (b) Shaffer, W. K. A.; Ray, W. H. *J. Appl. Polym. Sci.* **1997**, *65*, 1053. (c) Han-Adebekun, G. C.; Hamba, M.; Ray, W. H. *J. Polym. Sci. A: Polym. Chem.* **1997**, *35*, 2063. (d) Hamba, M.; Han-Adebekun, G. C.; Ray, W. H. *J. Polym. Sci. A: Polym. Chem.* **1997**, *35*, 2075.

(11) (a) Xu, J. T.; Feng, L. X.; Yang, S. L. *Macromol.* **1997**, *30*, 2539. (b) Xu, J. T.; Feng, L. X.; Yang, S. L.; Wu, Y. N.; Yang, Y. Q.; Kong, X. M. *Macromol. Rapid Commun.* **1996**, *17*, 645.

(12) (a) Fujimoto, H.; Koga, N.; Hataue, J. *J. Phys. Chem.* **1984**, *88*, 3539. (b) Fujimoto, H.; Yamasaki, T.; Mizutani, H.; Koga, N. *J. Am. Chem. Soc.* **1985**, *107*, 6157.

(13) (a) Shiga, A.; Kawamura-Kuribayashi, H.; Sasaki, T. *J. Mol. Catal.* **1995**, *98*, 15. (b) Shiga, A. *J. Macromol. Sci. A* **1997**, *34*, 1867.

(14) (a)Mosley, D. H.; Denil, C.; Champagne, B.; André J−M. *J. Mol. Catal. A* **1997**, *119*, 235. (b) Ferriera, M. L.; Juan, A.; Castellani, N. J.; Damiani, D. E. *J. Mol. Catal.* **1994**, *87*, 137. (c) Ferriera, M. L.; Castellani, N. J.; Damiani, D. E., Juan, A. *J. Mol. Catal. A* **1997**, *122*, 25. (d) Ferriera, M. L.; Marta Branda, M.; Juan, A.; Damiani, D. E. *J. Mol. Catal. A* **1997**, *122*, 51.

(15) Colbourn, E. A.; Cox, P. A.; Carruthers, B.; Jones, P. J. V. *J. Mater. Chem.* **1994**, *4*, 805.

(16) Gale, J. D.; Catlow, C. R. A.; Gillan, M. J. *Top. Catal.* **1999**, *9*, 235.

(17) (a) Boero, M.; Parrinello, M.; Terakura, K. *J. Am. Chem. Soc.* **1998**, *120*, 2746. (b) Boero, M.; Parrinello, M.; Terakura, K. *Surf. Sci.* **1999**, *438*, 1.

(18) Boero, M.; Parrinello, M.; Hüffer, S.; Wei*β*, H. *J. Am. Chem. Soc.* **2000**, *122*, 501.

(19) Kohn, W.; Sham, L. J. *Phys. Rev.* **1965**, *140*, A 1133; Jones, R. O.; Gunnarsson, O. *Rev. Mod. Phys.* **1989**, *61*, 689.

(20) (a) Becke, A. D. *Phys. Rev. A* **1988**, *38*, 3098. (b) Lee, C.; Yang, W.; Parr, R. G. *Phys. Rev. B* **1988**, *37*, 785.

(21) Car, R.; Parrinello, M. *Phys. Rev. Lett.* **1985**, *55*, 2471.

(22) We have used the code CPMD developed by J. Hutter, P. Ballone, M. Bernasconi, P. Focher, E. Fois, S. Goedecker, D. Marx, M. Parrinello, M. Tuckerman, at MPI für Festkörperforschung and IBM Zurich Research Laboratory (1990−1997). The code was ported on VPP − Fujitsu by M. Boero.

(23) The surfaces have been constructed by cleaving the bulk α-$MgCl_2$ according to the conventions of the Surface Builder of *Cerius*^{2} graphic package from MSI.

(24) Troullier, N.; Martins, J. L. *Phys. Rev. B* **1991**, *43*, 1993.

(25) Louie, S. G.; Froyen S.; Cohen, M. L. *Phys. Rev. B* **1982**, *26*, 1738.

(26) We enlarged the cutoff to 70 Ry, as against to the 40 Ry values of our previous works, to be consistent with calculations involving the donor phthalate, where oxygen atoms, requiring 70 Ry for a good convergence, are involved.

(27) See, e.g., (a) Sprik, M.; Hutter, J.; Parrinello, M. *J. Chem. Phys.* **1996**, *105*, 1142. (b) Boero, M.; Andreoni, W. *Chem. Phys. Lett.* **1997**, *265*, 24. (c) Balasubramanian, S.; Mundy, C. J.; Klein, M. L. *J. Phys. Chem. B* **1998**, *102*, 10136. (d) Silvestrelli, P. L.; Parrinello, M. *Phys. Rev. Lett.* **1999**, *82*, 3308. (e) Rousseau, R.; Boero, M.; Bernasconi, M.; Parrinello, M.; Terakura, K. *Phys. Rev. Lett.* **2000**, *85*, 1254. (f) Boero, M.; Morikawa, Y.; Terakura, K.; Ozeki, M. *J. Chem. Phys.* **2000**, *112*, 9549, and references therein.

(28) See, e.g., (a) Johnson, B. G.; Gill, P. M. W.; Pople, J. A. *J. Chem. Phys.* **1993**, *98*, 5612. (b) Pis-Diez, R. *Chem. Phys. Lett.* **1998**, *287*, 542. (c) Cohen, A. J.; Handy, N. C. *Chem. Phys. Lett.* **2000**, *316*, 160. (d) Ahlrichs, R.; Furche, F.; Grimme, S. *Chem. Phys. Lett.* **2000**, *325*, 317, and references therein.

(29) (a) Ciccotti, G.; Ferrario, M.; Hynes, J. T.; Kapral, R. *Chem. Phys.* **1989**, *129*, 241. (b) Carter, E. A.; Ciccotti, G.; Hynes, J. T.; Kapral, R. *Chem. Phys. Lett.* **1989**, *156*, 472. (c) Paci, E.; Ciccotti, G.; Ferrario, M.; Kapral, R. *Chem. Phys. Lett.* **1991**, *176*, 581. (d) Ciccotti, G.; Ferrario, M. Monte Carlo and Molecular Dynamics of Condensed Matter Systems. *Proceedings of Euroconference on Computer Simulation in Condensed Matter Physics and Chemistry*; Binder, K., Ciccotti, G., Eds.; SIF, Como, 1995.

(30) (a) Mülders, T.; Krüger, P.; Swegat, W.; Schlitter, J. *J. Chem. Phys.* **1996**, *104*, 4869. (b) den Otter, W. K.; Briels, W. J. *J. Chem. Phys.* **1998**, *109*, 4139. (c) Sprik, M.; Ciccotti, G. *J. Chem. Phys.* **1998**, *109*, 7737.

(31) Experimental crystallographic data from Dorrepaal, J. *J. Appl. Crystallogr.* **1984**, *17*, 483.

(32) See, e.g., *Gmelins Handbuch der Anorganischen Chemie*; Verlag Chemie GmbH: Weinheim, 1951.

(33) (a) Magni, E.; Somorjai, G. A. *Catal. Lett.* **1995**, *35*, 205. (b) Magni, E.; Somorjai, G. A. *Appl. Surf. Sci.* **1995**, *89*, 187. (c) Magni, E.; Somorjai, G. A. *Surf. Sci.* **1996**, *345*, 1. (d) Magni, E.; Somorjai, G. A. *J. Phys. Chem. B* **1998**, *102*, 8788. (e) Korányi, T. I.; Magni, E.; Somorjai, G. A. *Top. Catal.* **1999**, *7*, 179.

(34) Private communication of BASF AG to MPI−FKF.

(35) (a) Albizzati, E.; Giannini, U.; Morini, G.; Smith, C. A.; Ziegler, R. C. In *Ziegler Catalysts*; Fink, G., Mülhaupt, R., Brintzinger, H. H., Eds.; Springer-Verlag: Berlin, Heidelberg, 1995; p 413, and references therein. (b) Chadwick, J. C. *ibid.* p 427, and references therein. (c) Morini, G.; Albizzati, E.; Balbontin, G.; Mignozzi, I.; Sacchi, M. C.; Forlini, F.; Tritto, I. *Macromolecules* **1996**, *29*, 5770. (d) Albizzati, E.; Giannini, U.; Balbontin, G.; Camurati, I.; Chadwick, J. C.; Dall'Occo, T.; Dubitsky, Y.; Galimberti, M.; Morini, G.; Maldotti, A. *J. Polym. Sci.: Polymer Chem.* **1997**, *35*, 2645. (e) Toto, M.; Morini, G.; Guerra, G.; Corradini, P.; Cavallo, L. *Macromol.* **2000**, *33*, 1134.

(36) We report the relaxation energies in kcal per mole of Mg in order to simplify the comparison with supercells containing different amounts of $MgCl_2$ formula units.

(37) Terano, M. Private communication.

(38) Jones, P. J. V.; Oldman, R. J.; *Transition Metals and Organometallics as Catalysts for Olefin Polymerization*; Kaminsky, W., Sinn, H., Eds.; Springer-Verlag: Berlin, 1988; p 223.

(39) Private communication of BASF AG to MPI−FKF.

(40) Kissin, Y. V. *Isospecific Polymerization of Olefins*; Springer-Verlag: New York, 1985.

(41) Allen, G. B. *Comprehensive Polymer Science*; Pergamon Press: Oxford, 1989.

(42) (a) Brintzinger, H. H.; Fischer, D.; Mülhaupt, R.; Rieger, B.; Waymouth, R. M. *Angew. Chem. Int. Ed.* **1995**, *34*, 1143, and references therein. (b) Corradini, P.; Guerra, G.; Vacatalleo, M.; Villani, V. *Gazz. Chim. Ital.* **1988**, *118*, 173.

(43) (a) Becke, A. D.; Edgecombe, K. E. *J. Chem. Phys.* **1990**, *92*, 5397. (b) Savin, A.; Becke, A. D.; Flad, J.; Nesper, R.; Preuss, H.; von Schnering, H. G. *Angew. Chem.* **1991**, *103*, 421. (c) Savin, A.; Flad, H.; Flad, J.; Preuss, H.; von Schnering, H. G. *Angew. Chem.* **1992**, *104*, 185. (d) Silvi, B.; Savin, A. *Nature* **1994**, *371*, 683.

(44) (a) Ahlrichs, R.; Bär, M.; Häser, M.; Horn, H.; Kölmel, C. *Chem. Phys. Lett.* **1989**, *162*, 165. (b) Ahlrichs, R.; v. Arnim, M. *TURBOMOLE, Parallel Implementation of SCF, Density Functional, and Chemical Shift Modules*. In *Methods and Techniques in Computational Chemistry: METECC-95*, Clementi, E., Corongiu, G., Eds., 1995.